Crystal structure of paliperidone, $C_{23}H_{27}FN_4O_3$

James A. Kaduk,[1,a] Kai Zhong,[2] Amy M. Gindhart,[2] and Thomas N. Blanton[2]
[1]*Illinois Institute of Technology, 3101 S. Dearborn St., Chicago, Illinois 60616*
[2]*ICDD, 12 Campus Blvd., Newtown Square, Pennsylvania, 19073-3273*

(Received 12 December 2015; accepted 14 February 2016)

The crystal structure of paliperidone has been solved and refined using synchrotron X-ray powder diffraction data, and optimized using density functional techniques. Paliperidone crystallizes in space group $P2_1/n$ (# 14) with $a = 14.151\,58(6)$, $b = 21.537\,80(9)$, $c = 6.913\,26(2)$ Å, $\beta = 92.3176(2)°$, $V = 2105.396(13)$ Å^3, and $Z = 4$. The unit-cell volume at 295 K is 1.5% larger than at 200 K, but the expansion is anisotropic; the *b*-axis is nearly constant at the two temperatures, while the *a*- and *c*-axes expand by 0.71 and 0.87%, respectively. There is only one significant hydrogen (H)-bond in the crystal structure. This H-bond is between the hydroxyl group O31–H58 and the ketone oxygen O25. The result is a chain along the *c*-axis with graph set C1,1(7). In addition to this H-bond, the molecular packing is dominated by van der Waals attractions. The powder pattern is included in the Powder Diffraction File™ as entry 00-064-1497. © *2016 International Centre for Diffraction Data*. [doi:10.1017/S0885715616000087]

Key words: paliperidone, Invega, powder diffraction, Rietveld refinement, density functional theory

I. INTRODUCTION

Paliperidone (trade name Invega) is a benzisoxazole derivative and the principal active metabolite of risperidone. As a dopamine antagonist and serotonin type 2A antagonist of the atypical antipsychotic class of medications, it is approved for the treatment of schizophrenia (Dolder *et al.*, 2008). The systematic name (CAS Registry Number 144598-75-4) is (*RS*)-3-[2-[4-(6-fluorobenzo[*d*]isoxazol-3-yl)-1-piperidyl]ethyl]-7-hydroxy-4-methyl-1,5-diazabicyclo [4.4.0]deca-3,5-diene-2-one. A two-dimensional molecular diagram is shown in Figure 1.

The presence of high-quality reference powder patterns in the Powder Diffraction File (PDF; ICDD, 2014) is important for phase identification, particularly by pharmaceutical, forensic, and law enforcement scientists. The crystal structures of a significant fraction of the largest dollar volume pharmaceuticals have not been published and thus calculated powder patterns are not present in the PDF-4 databases. Sometimes experimental patterns are reported, but they are generally of low quality. This structure is a result of the collaboration among ICDD, Illinois Institute of Technology (IIT), Poly Crystallography Inc., and Argonne National Laboratory to measure high-quality synchrotron powder patterns of commercial pharmaceutical ingredients, include these reference patterns in the PDF, and determine the crystal structures of these active pharmaceutical ingredients (APIs).

Even when the crystal structure of an API is reported, the single-crystal structure was often determined at low temperature. Most powder measurements are performed at ambient conditions. Thermal expansion (often anisotropic) means that the peak positions calculated from a low-temperature single-crystal structure often differ significantly from those measured at ambient conditions. These peak shifts can result in failure of default search/match algorithms to identify a phase, even when it is present in the sample. High-quality reference patterns measured at ambient conditions are thus critical for easy identification of APIs using standard powder diffraction practices.

II. EXPERIMENTAL

Paliperidone was a commercial reagent, purchased from Santa Cruz Biotechnology, and was used as-received. The white powder was packed into a 1.5 mm diameter Kapton capillary and rotated during the measurement at ~50 cycles s^{-1}. The powder pattern was measured at 295 K at beam line 11-BM (Lee *et al.*, 2008; Wang *et al.*, 2008) of the Advanced Photon Source at Argonne National Laboratory using a wavelength of 0.413 891 Å from 0.5° to 50°2θ with a step size of 0.001° and a counting time of 0.1 s step^{-1}. The pattern was indexed using Jade 9.5 (MDI, 2014) on a primitive monoclinic unit cell having $a = 14.153$, $b = 21.534$, $c = 6.913$ Å, $\beta = 92.3°$, and $V = 2105.1$ Å^3. The space group was suggested to be $P2_1/n$, which is consistent with the racemic nature of commercial material. The unit-cell volume is

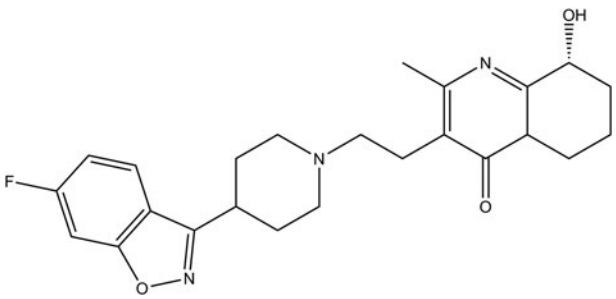

Figure 1. The molecular structure of paliperidone.

[a]Author to whom correspondence should be addressed. Electronic mail: kaduk@polycrystallography.com

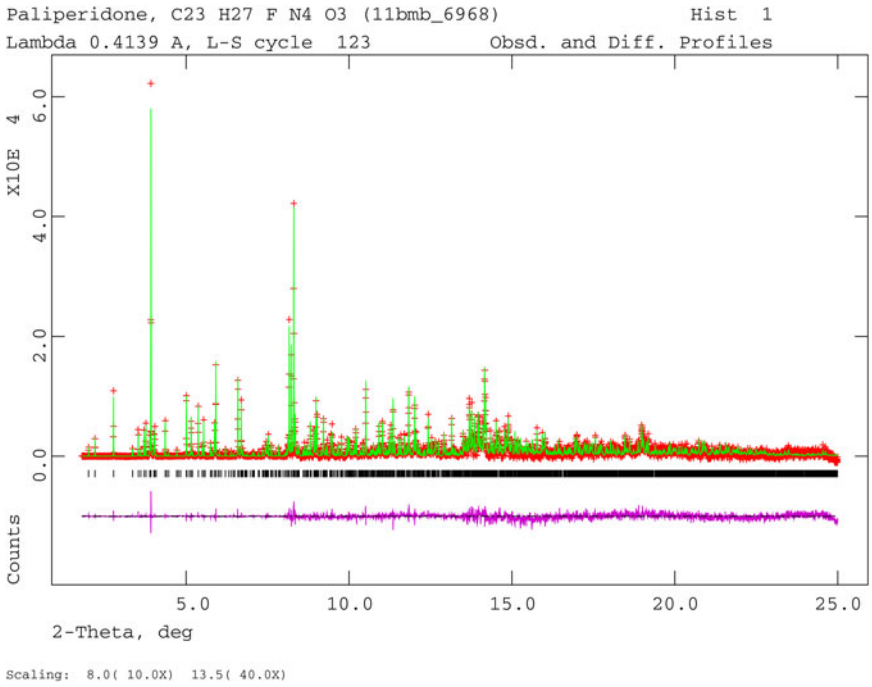

Figure 2. (Color online) The Rietveld plot for the refinement of paliperidone. The red crosses represent the observed data points, and the green line is the calculated pattern. The magenta curve is the difference pattern, plotted at the same vertical scales as the other patterns. The vertical scale has been multiplied by a factor of 10 for $2\theta > 8.0°$, and by a factor of 40 for $2\theta > 13.5°$.

TABLE I. Rietveld refined crystal structure of paliperidone.

Crystal data	
$C_{23}H_{27}FN_4O_3$	$\beta = 92.3176\ (2)°$
$M_r = 426.49$	$V = 2105.396\ (13)$ Å^3
Monoclinic, $P2_1/n$	$Z = 4$
$a = 14.151\ 58\ (6)$ Å	synchrotron radiation, $\lambda = 0.413\ 891$ Å
$b = 21.537\ 80\ (9)$ Å	$T = 295$ K
$c = 6.913\ 26\ (2)$ Å	Cylinder, 1.5×1.5 mm^2
Data collection	
11-BM APS diffractometer	Scan method: step
Specimen mounting: Kapton capillary	$2\theta_{min} = 0.5°$, $2\theta_{max} = 50°$, $2\theta_{step} = 0.001°$
Data collection mode: transmission	
Refinement	
Least-squares matrix: full	49 494 data points
$R_p = 0.070$	Profile function: CW Profile function number 4 with 21 terms Pseudovoigt profile coefficients as parameterized in Thompson *et al.* (1987). Asymmetry correction of Finger *et al.* (1994). Microstrain broadening by Stephens (1999). #1(GU) = 1.163 #2(GV) = −0.126 #3(GW) = 0.063 #4(GP) = 0.000 #5(LX) = 0.173 #6(ptec) = 0.00 #7(trns) = 0.00 #8(shft) = 0.0000 #9(sfec) = 0.00 #10 (S/L) = 0.0011 #11(H/L) = 0.0011 #12(eta) = 0.9999 #13(S400) = 6.4×10^{-3} #14(S040) = 6.4×10^{-4} #15(S004) = 1.5×10^{-2} #16(S220) = -1.2×10^{-3} #17 (S202) = 8.0×10^{-3} #18(S022) = 2.5E × 10^{-4} #19(S301) = 7.3×10^{-3} #20 (S103) = 9.5×10^{-3} #21(S121) = -7.2×10^{-4} Peak tails are ignored where the intensity is below 0.0010 times the peak Aniso. broadening axis 0.0 0.0 1.0
$R_{wp} = 0.086$	111 parameters
$R_{exp} = 0.055$	83 restraints
$R(F^2) = 0.144\ 74$	$(\Delta/\sigma)_{max} = 0.01$
$\chi^2 = 2.496$	Background function: GSAS Background function number 1 with 9 terms. Shifted Chebyshev function of 1st kind 1: 172.040 2: −17.5917 3: −6.631 44 4: 12.4497 5: −16.2031 6: −0.506 910 7: 7.177 38 8: −4.726 95 9: 15.9990

Fractional atomic coordinates and isotropic or equivalent isotropic displacement parameters (Å^2)

	x	y	z	U_{iso}
C1	0.3012 (5)	0.3910 (3)	0.6933 (8)	0.0660 (9)
C2	0.3278 (5)	0.3453 (4)	0.8126 (9)	0.0660 (9)
C3	0.4006 (5)	0.3099 (3)	0.7485 (9)	0.0660 (9)

Continued

https://doi.org/10.1017/S0885715616000087 Published online by Cambridge University Press

TABLE I. Continued

Fractional atomic coordinates and isotropic or equivalent isotropic displacement parameters (Å^2)				
	x	y	z	U_{iso}
C4	0.4521 (5)	0.3244 (4)	0.5919 (10)	0.0660 (9)
C5	0.4183 (5)	0.3654 (4)	0.4577 (8)	0.0660 (9)
C6	0.3417 (5)	0.4034 (4)	0.5158 (9)	0.0660 (9)
F7	0.4317 (3)	0.2665 (2)	0.8772 (5)	0.0660 (9)
O8	0.2237 (3)	0.4300 (2)	0.7046 (6)	0.0660 (9)
N9	0.2224 (4)	0.4710 (2)	0.5420 (7)	0.0660 (9)
C10	0.2914 (4)	0.4552 (3)	0.4383 (8)	0.0660 (9)
C11	0.3072 (5)	0.4882 (3)	0.2481 (7)	0.0510 (10)
C12	0.3992 (4)	0.5250 (4)	0.2560 (8)	0.0510 (10)
C13	0.4122 (5)	0.5620 (3)	0.0597 (9)	0.0510 (10)
N14	0.3358 (4)	0.6046 (3)	0.0282 (7)	0.0510 (10)
C15	0.2478 (5)	0.5677 (3)	0.0090 (9)	0.0510 (10)
C16	0.2251 (4)	0.5337 (3)	0.1921 (9)	0.0510 (10)
C17	0.3494 (4)	0.6426 (3)	−0.1499 (8)	0.0379 (18)
C18	0.2861 (4)	0.7002 (3)	−0.1614 (8)	0.0379 (18)
C19	0.3242 (4)	0.7496 (3)	−0.0303 (6)	0.0397 (7)
C20	0.2945 (4)	0.7595 (3)	0.1525 (6)	0.0397 (7)
N21	0.3280 (4)	0.8072 (3)	0.2702 (6)	0.0397 (7)
C22	0.3983 (4)	0.8395 (3)	0.2070 (7)	0.0397 (7)
N23	0.4299 (4)	0.8341 (3)	0.0234 (6)	0.0397 (7)
C24	0.3951 (5)	0.7876 (3)	−0.1034 (7)	0.0397 (7)
O25	0.4275 (3)	0.7824 (2)	−0.2640 (6)	0.0397 (7)
C26	0.2157 (5)	0.7256 (3)	0.2378 (8)	0.0397 (7)
C27	0.4412 (4)	0.8889 (3)	0.3447 (8)	0.0397 (7)
C28	0.5017 (5)	0.9360 (3)	0.2425 (8)	0.0397 (7)
C29	0.5664 (4)	0.9041 (3)	0.1066 (8)	0.0397 (7)
C30	0.5090 (5)	0.8722 (3)	−0.0510 (8)	0.0397 (7)
O31	0.5032 (4)	0.8547 (3)	0.4661 (7)	0.103 (2)
H32	0.283 34	0.334 54	0.953 45	0.0858 (11)
H33	0.501 97	0.285 77	0.560 58	0.0858 (11)
H34	0.454 09	0.372 52	0.337 96	0.0858 (11)
H35	0.315 78	0.453 86	0.141 74	0.0662 (13)
H36	0.398 38	0.561 07	0.3827	0.0662 (13)
H37	0.461 86	0.496 39	0.2975	0.0662 (13)
H38	0.423 74	0.525 67	−0.041 68	0.0662 (13)
H39	0.480 47	0.588 04	0.0835	0.0662 (13)
H40	0.248 11	0.5349	−0.115 33	0.0662 (13)
H41	0.189 09	0.600 26	−0.022 92	0.0662 (13)
H42	0.217 25	0.567 07	0.309 05	0.0662 (13)
H43	0.160 74	0.507 57	0.174 52	0.0702 (13)
H44	0.341 57	0.609 18	−0.281 26	0.049 (2)
H45	0.425 91	0.653 59	−0.145 44	0.049 (2)
H46	0.2936	0.713 71	−0.318 15	0.049 (2)
H47	0.215 66	0.685 28	−0.146 64	0.049 (2)
H48	0.243 42	0.677 45	0.283 38	0.0516 (9)
H49	0.156 37	0.710 55	0.125 66	0.0516 (9)
H50	0.183 62	0.745 63	0.353 74	0.0516 (9)
H51	0.386 91	0.904 16	0.428 57	0.0516 (9)
H52	0.448 13	0.966 35	0.163 07	0.0516 (9)
H53	0.536 52	0.963 81	0.352 98	0.0516 (9)
H54	0.610 55	0.873 04	0.181 26	0.0516 (9)
H55	0.609 57	0.940 79	0.038 35	0.0516 (9)
H56	0.472 52	0.905 62	−0.155 94	0.0516 (9)
H57	0.551 56	0.842 64	−0.141 45	0.0516 (9)
H58	0.474 85	0.826 37	0.557 73	0.134 (3)

consistent with $Z = 4$. After solution and refinement of the structure, a reduced cell search in the Cambridge Structural Database (Allen, 2002) yielded Refcode YAGRIJ for paliperidone (Betz *et al.*, 2011).

The structure in this study was solved by direct methods (including the Resolution Bias Modification) using EXPO2009 (Altomare *et al.*, 2009). The Rietveld refinement was carried out using General Structure Analysis System (GSAS) (Larson and Von Dreele, 2004). Only the 1.8°–25.0° portion of the pattern was included in the refinement ($d_{min} = 0.96$ Å). All non-H-bond distances and angles were subjected to restraints, based on a Mercury/Mogul Geometry

https://doi.org/10.1017/S0885715616000087 Published online by Cambridge University Press

TABLE II. DFT-optimized (CRYSTAL09) crystal structure of paliperidone.

Crystal data	
$C_{23}H_{27}FN_4O_3$	$\beta = 92.3176°$
$M_r = 426.49$	$V = 2105.40$ Å^3
Monoclinic, $P2_1/n$	$Z = 4$
$a = 14.151\,58$ Å	
$b = 21.537\,80$ Å	
$c = 6.913\,26$ Å	

Fractional atomic coordinates and isotropic displacement parameters (Å^2)

	x	y	z	U_{iso}
C1	0.296 96	0.392 09	0.695 61	0.0660
C2	0.322 13	0.344 64	0.824 85	0.0660
C3	0.397 61	0.309 14	0.767 20	0.0660
C4	0.446 17	0.317 82	0.596 11	0.0660
C5	0.418 70	0.365 94	0.472 54	0.0660
C6	0.343 26	0.403 98	0.524 47	0.0660
F7	0.426 19	0.261 00	0.884 59	0.0660
O8	0.224 13	0.432 21	0.712 88	0.0660
N9	0.222 07	0.471 97	0.549 19	0.0660
C10	0.291 42	0.455 66	0.440 27	0.0660
C11	0.308 32	0.489 42	0.254 45	0.0510
C12	0.401 43	0.526 97	0.265 36	0.0510
C13	0.415 02	0.560 84	0.073 67	0.0510
N14	0.336 14	0.602 57	0.025 65	0.0510
C15	0.247 02	0.567 79	0.007 37	0.0510
C16	0.227 05	0.533 21	0.1935 4	0.0510
C17	0.352 06	0.638 31	−0.149 97	0.0397
C18	0.289 51	0.696 68	−0.169 72	0.0397
C19	0.323 21	0.747 72	−0.035 20	0.0397
C20	0.290 20	0.759 49	0.145 92	0.0397
N21	0.327 43	0.805 75	0.262 42	0.0397
C22	0.397 12	0.839 44	0.200 15	0.0397
N23	0.432 25	0.832 50	0.020 21	0.0397
C24	0.397 26	0.786 14	−0.105 95	0.0397
O25	0.430 47	0.779 84	−0.269 37	0.0397
C26	0.213 25	0.721 53	0.231 68	0.0397
C27	0.444 06	0.884 95	0.344 11	0.0397
C28	0.497 88	0.936 03	0.243 53	0.0397
C29	0.564 50	0.906 00	0.102 83	0.0397
C30	0.507 53	0.872 61	−0.056 05	0.0397
O31	0.509 88	0.852 08	0.466 31	0.1034
H32	0.283 34	0.334 54	0.953 45	0.0858
H33	0.501 97	0.285 77	0.560 58	0.0858
H34	0.454 09	0.372 52	0.337 96	0.0858
H35	0.315 78	0.453 86	0.141 74	0.0662
H36	0.398 38	0.561 07	0.382 70	0.0662
H37	0.461 86	0.496 39	0.297 50	0.0662
H38	0.423 74	0.525 67	−0.041 68	0.0662
H39	0.480 47	0.588 04	0.083 50	0.0662
H40	0.248 11	0.534 90	−0.115 33	0.0662
H41	0.189 09	0.600 26	−0.022 92	0.0662
H42	0.217 25	0.567 07	0.309 05	0.0662
H43	0.160 74	0.507 57	0.174 52	0.0702
H44	0.341 57	0.609 18	−0.281 26	0.0493
H45	0.425 91	0.653 59	−0.145 44	0.0493
H46	0.293 60	0.713 71	−0.318 15	0.0493
H47	0.215 66	0.685 28	−0.146 64	0.0493
H48	0.243 42	0.677 45	0.283 38	0.0516
H49	0.156 37	0.710 55	0.125 66	0.0516
H50	0.183 62	0.745 63	0.353 74	0.0516
H51	0.386 91	0.904 16	0.428 57	0.0516
H52	0.448 13	0.966 35	0.163 07	0.0516
H53	0.536 52	0.963 81	0.352 98	0.0516
H54	0.610 55	0.873 04	0.181 26	0.0516
H55	0.609 57	0.940 79	0.038 35	0.0516
H56	0.472 52	0.905 62	−0.155 94	0.0516
H57	0.551 56	0.842 64	−0.141 45	0.0516
H58	0.474 85	0.826 37	0.557 73	0.1344

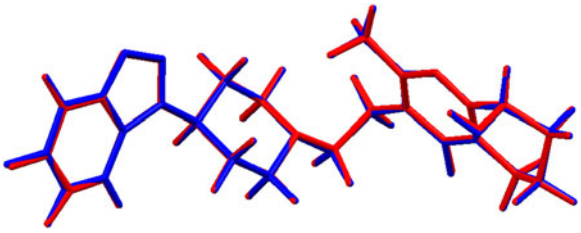

Figure 3. (Color online) Comparison of the refined and optimized structures of paliperidone. The Rietveld refined structure is colored red, and the DFT-optimized structure is in blue.

Check (Bruno *et al.*, 2004; Sykes *et al.*, 2011) of the molecule. The Mogul average and standard deviation for each quantity were used as the restraint parameters. The restraints contributed 3.31% to the final χ^2. Isotropic displacement coefficients were refined, grouped by chemical similarity. The hydrogen atoms were included in calculated positions (Materials Studio; Accelrys, 2013), which were recalculated during the refinement. The U_{iso} of each hydrogen atom was constrained to be 1.3× that of the heavy atom to which it is attached. The peak profiles were described using profile function #4 (Thompson *et al.*, 1987; Finger *et al.*, 1994), which includes the Stephens (1999) anisotropic strain broadening model. The background was modeled using a nine-term shifted Chebyshev polynomial. The final refinement of 111 variables using 23 282 observations yielded the residuals $R_{wp} = 0.086$, $R_p = 0.070$, and $\chi^2 = 2.496$. The largest peak (1.24 Å from C26) and hole (0.29 Å from F7) in the difference Fourier map were 0.48 and −0.68 e (Å)$^{-3}$, respectively. The Rietveld plot is included as Figure 2. The largest errors are in the positions of the low-angle peaks, and may reflect subtle changes in the specimen during the measurement.

The single crystal structure YAGRIJ has the hydroxyl group (in our numbering) C27–O31–H58 disordered over two positions, with occupancies 0.86 and 0.14. In addition, the methyl hydrogens H48, H49, and H50 are disordered over two positions. Refinement of this disordered model (126 variables) using the same strategy yielded the residuals $R_{wp} = 0.086$, $R_p = 0.070$, and $\chi^2 = 2.526$. While it is impossible to know if the single crystal and powder samples were exactly the same, this result points out that it may be difficult to detect small levels of disorder using powder data, even synchrotron powder data.

A density functional geometry optimization (fixed experimental unit cell) was carried out using CRYSTAL09 (Dovesi *et al.*, 2005). The basis sets for the H, C, N, and O atoms were those of Gatti *et al.* (1994), and the basis set for F was that of Nada *et al.* (1993). The calculation used eight k-points and the B3LYP functional, and took ∼15 days on a 3.0 GHz PC.

III. RESULTS AND DISCUSSION

The refined atom coordinates of paliperidone are reported in Table I, and the coordinates from the density functional theory (DFT) optimization in Table II. The root-mean-square deviation of the non-hydrogen atoms is 0.068 Å, and the maximum deviation is 0.154 Å, at C43 (Figure 3). The excellent agreement between the refined and optimized structures is strong evidence that the structure is correct (van de Streek and Neumann, 2014). The discussion of the geometry uses

https://doi.org/10.1017/S0885715616000087 Published online by Cambridge University Press

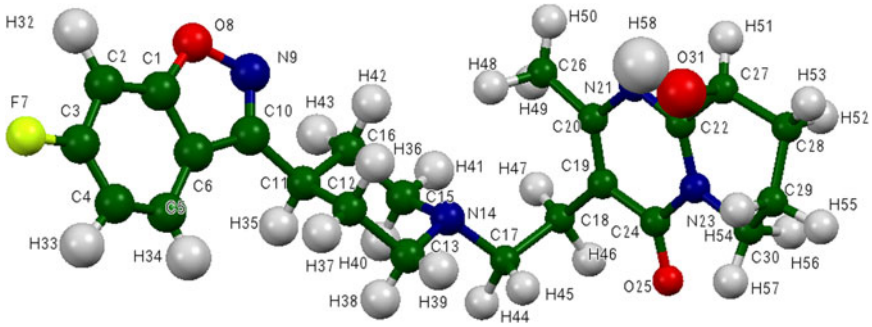

Figure 4. (Color online) The molecular structure of paliperidone, with the atom numbering. The atoms are represented by 50% probability spheroids.

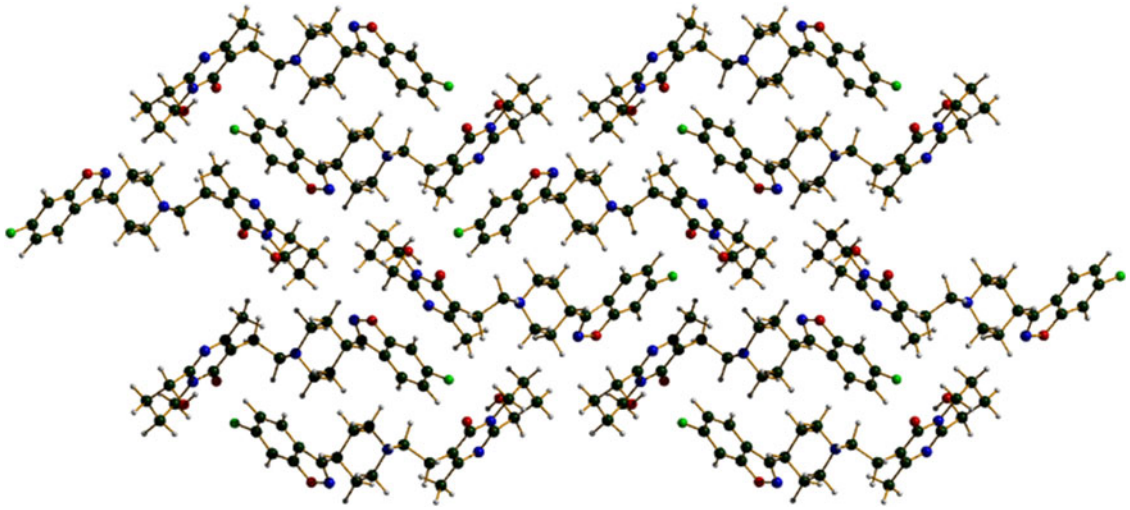

Figure 5. (Color online) The crystal structure of paliperidone, viewed down the *c*-axis.

the DFT-optimized structure. The asymmetric unit (with atom numbering) is illustrated in Figure 4, and the crystal structure is presented in Figure 5.

All the bond distances, angles, and torsion angles fall within the normal ranges indicated by a Mercury Mogul Geometry Check. A Mercury Molecule Overlay of the current structure and the single-crystal structure YAGRIJ failed, because the hydroxyl group O31–H58 (in our numbering) is disordered 86/14% over two positions in the single-crystal structure. The displacement coefficient of O31 is much higher than that of the other atoms, suggesting that disorder is also present in the room-temperature powder structure. A Mercury Structure Overlay indicated that the root-mean-square difference between the two molecules was only 0.033 Å, and thus the expansion between 200 and 295 K involves intermolecular separations.

A quantum mechanical (DFT/B3LYP functional/6-31G* basis set/vacuum) energy analysis using Spartan '14 (Wavefunction, 2013) suggests that the observed conformation is with 3.4 kcal mole^{-1} of a local minimum. A molecular mechanics (MMFF) conformational analysis indicates that the observed conformation is 43.08 kcal mole^{-1} higher in energy than the minimum-energy conformation, which curls up on itself to generate parallel stacking of the fused ring systems. This difference in energy indicates that intermolecular interactions are important in determining the solid-state conformation.

Determination of the single-crystal structure at 200 K and the powder structure at 295 K provides an opportunity to assess the thermal expansion of paliperidone. The lattice parameters (transformed into the current $P2_1/n$ setting) are reported in Table III. The unit-cell volume at 295 K is 1.5% larger than at 200 K, but the expansion is anisotropic. The *b*-axis is nearly constant at the two temperatures, while the *a*- and *c*-axes expand by 0.71 and 0.87%, respectively, from 200 to 295 K. Comparison of the observed powder pattern with that calculated from YAGRIJ (Figure 6) shows that the positions of some peaks differ significantly. Some of the differences are large enough that a room-temperature powder diffraction pattern would not be identified as paliperidone in a default search/match, even if a pattern calculated from YAGRIJ were present in the PDF. The differences provide strong evidence for the desirability of including high-quality ambient-condition patterns in the PDF™.

There is only one significant hydrogen bond in the crystal structure of paliperidone (Table IV). This H-bond is between the hydroxyl group O31–H58 and the ketone oxygen O25. The result is a chain along the *c*-axis with graph set C1,1(7) (Etter, 1990; Bernstein *et al.*, 1995; Shields *et al.*, 2000). Using the correlation between the H···Acceptor distance for O–H···O hydrogen bonds developed by Rammohan, A. and Kaduk, J. A. (2016, Unpublished data), this hydrogen bond contributes 12.6 kcal mole^{-1} to the crystal energy. In the single-crystal structure YAGRIJ, the major occupancy hydrogen bond corresponds to 12.6 kcal mole^{-1}, while the minor occupancy orientation is reasonable for two hydrogen bonds with energies of 6.9 and 4.9 kcal mole^{-1}. The multiple potential hydrogen bonds and their relative energies may explain

https://doi.org/10.1017/S0885715616000087 Published online by Cambridge University Press

TABLE III. Lattice parameters of paliperidone; space group $P2_1/n$.

Temperature (K)	200	295	295/200
Source	YAGRIJ (Betz *et al.*, 2011)	This work	
a (Å)	14.051	14.151 58 (6)	1.0071
b (Å)	21.5613 (5)	21.537 80 (9)	0.9989
c (Å)	6.8537 (1)	6.913 26 (2)	1.0087
β (°)	92.637	92.3176 (2)	
V (Å^3)	2074.15 (7)	2105.396 (13)	1.0150

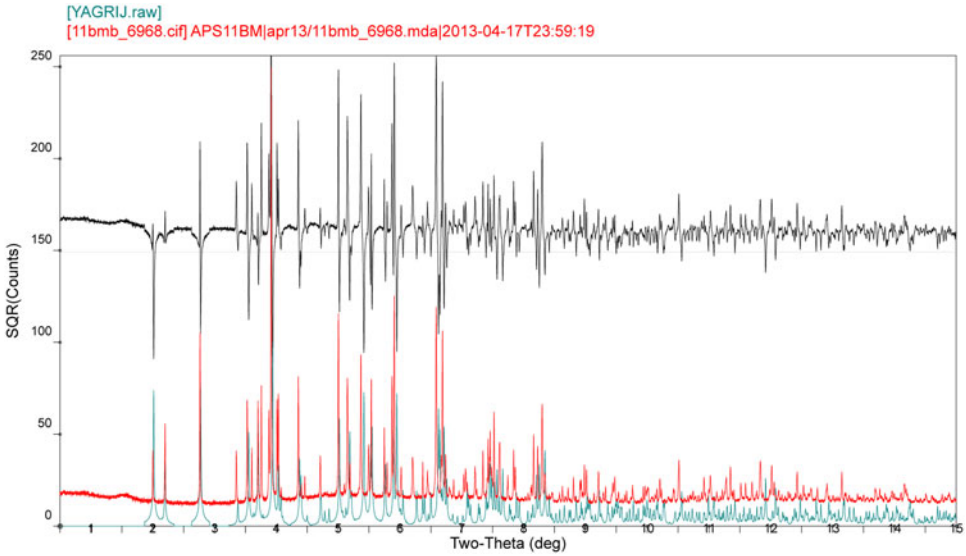

Figure 6. (Color online) Comparison of the observed 295 K powder pattern of paliperidone (red) with the pattern calculated from the 200 K structure in YAGRIJ (cyan). The black curve is the difference, and indicates the significant peak shifts between the two temperatures.

TABLE IV. Hydrogen bonds in paliperidone.

D–H···A	D–H (Å)	H···A (Å)	D···A (Å)	D–H···A (°)	Overlap (e)
O31–H58···O25	0.989	1.699	2.681	171.6	0.056
C25–H50···F7	1.089	2.454	3.475	155.6	0.008
C30–H57···O25	1.088	2.329	2.688	97.0	0.008

the disorder in the single-crystal structure. A very weak intermolecular C25–H50···F7 hydrogen bond may contribute to the crystal packing, and an intramolecular C30–H57···O25 hydrogen bond may influence the conformation of the molecule.

The volume of the Hirshfeld surface (Figure 7; Hirshfeld, 1977; McKinnon *et al.*, 2004; Spackman and Jayatilaka, 2009; Wolff *et al.*, 2012) is 518.54 Å^3, 98.52% of one-fourth the unit-cell volume (526.349 Å^3). The molecules are thus not tightly packed. The only significant close contacts (red in Figure 7) involve the O–H···O hydrogen bonds. An analysis of the contributions to the total crystal energy using the Forcite module of Materials Studio (Accelrys, 2013) suggests that angle distortion terms are a major intramolecular contribution to the crystal energy, and that van der Waals interactions dominate the intermolecular forces.

The Bravais–Friedel–Donnay–Harker (Bravais, 1866; Friedel, 1907; Donnay and Harker, 1937) morphology suggests that we might expect an elongated morphology for paliperidone, with {001} as the long axis. A second-order spherical harmonic preferred orientation model was included in the refinement; the texture index was 1.043, indicating a small but significant preferred orientation in this rotated capillary specimen.

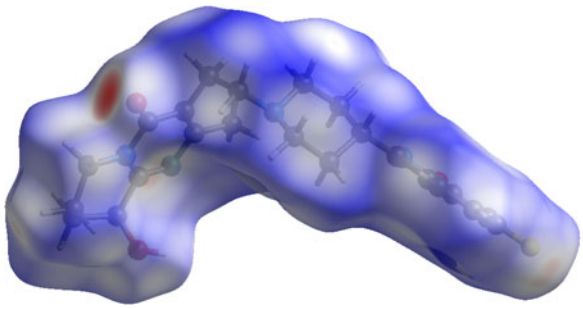

Figure 7. (Color online) The Hirshfeld surface of paliperidone. Intermolecular contacts longer than the sums of van der Waals radii are colored blue, and contacts shorter than the sums of the radii are colored red. Contacts equal to the sums of the radii are white.

https://doi.org/10.1017/S0885715616000087 Published online by Cambridge University Press

The powder pattern of paliperidone is included in the PDF as entry 00-064-1497.

SUPPLEMENTARY MATERIAL

To view supplementary material for this article, please visit http://dx.doi.org/10.1017/S0885715616000087

ACKNOWLEDGEMENTS

The use of the Advanced Photon Source at Argonne National Laboratory was supported by the U. S. Department of Energy, Office of Science, Office of Basic Energy Sciences, under Contract No. DE-AC02-06CH11357. This work was partially supported by the International Centre for Diffraction Data. We thank Lynn Ribaud for his assistance in data collection.

Accelrys (**2013**). *Materials Studio 7.0* (Accelrys Software Inc., San Diego, CA).

Allen, F. H. (**2002**). "The Cambridge Structural Database: a quarter of a million crystal structures and rising," Acta Crystallogr., B: Struct. Sci. **58**, 380–388.

Altomare, A., Camalli, M., Cuocci, C., Giacovazzo, C., Moliterni, A., and Rizzi, R. (**2009**). "EXPO2009: structure solution by powder data in direct and reciprocal space," J. Appl. Crystallogr. **42**(6), 1197–1202.

Bernstein, J., Davis, R. E., Shimoni, L., and Chang, N. L. (**1995**). "Patterns in hydrogen bonding: functionality and graph set analysis in crystals," Angew. Chem. Int. Ed. Engl., **34**(15), 1555–1573.

Betz, R., Gerber, T., Hosten, E., Dayananda, A. S., Yathirajan, H. S., and Thomas, S. (**2011**). "Paliperidone: 3-{2-[4-(6-fluoro-1,2-benzoxazol-3-yl)piperidin-1-yl]ethyl}−9-hydroxy-2-methyl-1,6,7,8,9,9a-hexahydropyrido [1,2-*a*]pyrimidin-4-one," Acta Crystallogr. E **67**, o2945–o2946; CSD Refcode YAGRIJ.

Bravais, A. (**1866**). *Etudes Cristallographiques* (Gauthier Villars, Paris).

Bruno, I. J., Cole, J. C., Kessler, M., Luo, J., Motherwell, W. D. S., Purkis, L. H., Smith, B. R., Taylor, R., Cooper, R. I., Harris, S. E., and Orpen, A. G. (**2004**). "Retrieval of crystallographically-derived molecular geometry information," J. Chem. Inf. Sci. **44**, 2133–2144.

Dolder, C., Nelson, M., and DeyoAm, Z. (**2008**). "Paliperidone for schizophrenia," Am. J. Health-Syst. Pharm. **65**(5), 403–413.

Donnay, J. D. H. and Harker, D. (**1937**). "A new law of crystal morphology extending the law of Bravais," Am. Mineral. **22**, 446–467.

Dovesi, R., Orlando, R., Civalleri, B., Roetti, C., Saunders, V. R., and Zicovich-Wilson, C. M. (**2005**). "CRYSTAL: a computational tool for the *ab initio* study of the electronic properties of crystals," Z. Kristallogr. **220**, 571–573.

Etter, M. C. (**1990**). "Encoding and decoding hydrogen-bond patterns of organic compounds," Acc. Chem. Res. **23**(4), 120–126.

Finger, L. W., Cox, D. E., and Jephcoat, A. P. (**1994**). "A correction for powder diffraction peak asymmetry due to axial divergence," J. Appl. Crystallogr. **27**(6), 892–900.

Friedel, G. (**1907**). "Etudes sur la loi de Bravais," Bull. Soc. Fr. Mineral. **30**, 326–455.

Gatti, C., Saunders, V. R., and Roetti, C. (**1994**). "Crystal-field effects on the topological properties of the electron-density in molecular crystals – the case of urea," J. Chem. Phys. **101**, 10686–10696.

Hirshfeld, F. L. (**1977**). "Bonded-atom fragments for describing molecular charge densities," Theor. Chem. Acta **44**, 129–138.

ICDD (**2014**). PDF-4+ 2014 (Database), International Centre for Diffraction Data, edited by Dr. Soorya Kabekkodu, Newtown Square, PA, USA.

Larson, A. C. and Von Dreele, R. B. (**2004**). *General Structure Analysis System (GSAS)* (Los Alamos National Laboratory Report LAUR 86-784).

Lee, P. L., Shu, D., Ramanathan, M., Preissner, C., Wang, J., Beno, M. A., Von Dreele, R. B., Ribaud, L., Kurtz, C., Antao, S. M., Jiao, X., and Toby, B. H. (**2008**). "A twelve-analyzer detector system for high-resolution powder diffraction," J. Synchrotron Radiat. **15**(5), 427–432.

McKinnon, J. J., Spackman, M. A., and Mitchell, A. S. (**2004**). "Novel tools for visualizing and exploring intermolecular interactions in molecular crystals," Acta Crystallogr. B **60**, 627–668.

MDI (**2014**). *Jade 9.5* (Materials Data. Inc., Livermore, CA).

Nada, R., Catlow, C. R. A., Pisani, C., and Orlando, R. (**1993**). "Ab initio Hartree–Fock perturbed-cluster study of neutral defects in LiF," Model. Simul. Mater. Sci. Eng. **1**, 165–187.

Shields, G. P., Raithby, P. R., Allen, F. H., and Motherwell, W. S. (**2000**). "The assignment and validation of metal oxidation states in the Cambridge Structural Database," Acta Crystallogr., B: Struct. Sci. **56** (3), 455–465.

Spackman, M. A. and Jayatilaka, D. (**2009**). "Hirshfeld surface analysis," CrystEngComm **11**, 19–32.

Stephens, P. W. (**1999**). "Phenomenological model of anisotropic peak broadening in powder diffraction," J. Appl. Crystallogr. **32**, 281–289.

Sykes, R. A., McCabe, P., Allen, F. H., Battle, G. M., Bruno, I. J. and Wood, P. A. (**2011**). "New software for statistical analysis of Cambridge Structural Database data," J. Appl. Crystallogr. **44**, 882–886.

Thompson, P., Cox, D. E., and Hastings, J. B. (**1987**). "Rietveld refinement of Debye-Scherrer synchrotron X-ray data from Al_2O_3," J. Appl. Crystallogr. **20**(2), 79–83.

van de Streek, J. and Neumann, M. A. (**2014**). "Validation of molecular crystal structures from powder diffraction data with dispersion-corrected density functional theory (DFT-D)," Acta Crystallogr., B: Struct. Sci., Cryst. Eng. Mater. **70**(6), 1020–1032.

Wang, J., Toby, B. H., Lee, P. L., Ribaud, L., Antao, S. M., Kurtz, C., Ramanathan, M., Von Dreele, R. B., and Beno, M. A. (**2008**). "A dedicated powder diffraction beamline at the Advanced Photon Source: commissioning and early operational results," Rev. Sci. Instrum. **79**, 085105.

Wavefunction, Inc. (**2013**). Spartan '14 version 1.1.0 (Wavefunction Inc.), 18401 Von Karman Ave., Suite 370, Irvine CA 92612.

Wolff, S. K., Grimwood, D. J., McKinnon, M. J., Turner, M. J., Jayatilaka, D., and Spackman, M. A. (**2012**). CrystalExplorer version 3.1 (University of Western Australia).